La Metallurgia Italiana
International Journal of the Italian Association for Metallurgy

Study of nitrogen effect on the mechanical alloying process and subsequent heat treatment of Fe-14 wt.% Mn powders

A. Guzmán, C. Peralta, F. González, E. Araya, D. Muranda, C. Aguilar, D. Guzmán

In the present work, the effect of nitrogen on the mechanical alloying process and subsequent heat treatment of Fe-14 wt.% Mn powders was studied. The mechanical alloying was carried out in a SPEX 8000D mill under Ar and N_2 atmospheres. The microstructural and morphological characterization of the powders was determined through X-ray diffraction and scanning electron microscopy. The study of the thermal stability of the mechanically alloyed powders was conducted utilizing differential scanning calorimetry. The results indicated that the milling atmosphere does not influence the phases detected after 10 h of mechanical alloying. After this milling time, the presence of two solid **α** Fe-Mn solutions with different manganese content was observed. In terms of morphology, powders milled under Ar atmosphere presented a more lamellar aspect than powders milled in a N_2 atmosphere. Regarding the distribution of sizes, it was determined that at initial milling times, a relative increase in the size of the agglomerates occurs as a result of the prevalence of the weld over the fracture. This trend is reversed to higher milling times. Concerning the study of thermal stability of the mechanical alloyed powders, it was determined that N_2 favors the formation of the **γ** Fe-Mn phase.

KEYWORDS: Fe-Mn ALLOYS, MECHANICAL ALLOYING, NITROGEN, THERMAL ANALYSIS, X-RAY DIFFRACTION

INTRODUCTION

High-Mn steels are the base of an important group of engineering materials with outstanding mechanical properties. The first of this type of steels was patented in 1883 by Sir Robert Hadfield [1]. These steels containing approximately 1.1 - 1.4 wt.% C and 11 - 14 wt.% Mn are characterized by a high work hardening capacity and a good balance between toughness and abrasion resistance. At present, Hadfield steels are widely used in various industries such as cement, mining, road construction, and railways [2, 3]. Another family of high-Mn steels of great importance today are the twinning–induced–plasticity (TWIP) steels, broadly used in the automotive industry due to their excellent impact properties, which are desirable for improving passenger safety performance and environmental standards [4]. Finally, shape memory allows (SMA) are a new class of Fe-Mn-based materials that would be of great relevance in the future. The shape-

Alexis Guzmán, Camila Peralta, Felipe González, Emilio Araya, Diego Muranda, Danny Guzmán
Departamento de Ingeniería en Metalurgia, Universidad de Atacama, Chile

Claudio Aguilar
Departamento de Ingeniería Metalúrgica y de Materiales, Universidad Técnica Federico Santa María, Chile

danny.guzman@uda.cl

memory effect of the Fe-Mn-based alloys is associated with deformation-induced martensitic transformation from γ-austenite with a face-centered cubic structure to ε-martensite with a hexagonal close-packed (HCP) structure, and its reversion on subsequent heating. The application of these alloys has been studied in different uses such as a fatigue-resistant seismic damping alloy, locking rings for bicycle frame pipes, crane rail joint plates, among others [5].

It is important to note that despite being discovered more than a hundred years ago, micro-deformation mechanisms of high manganese steels, especially its unusually high work hardening capacity, are still being subject to scientific studies [6].

The high work hardening behavior of these steels has been attributed to the interstitial solution of C, twinning, and deformation by slipping [7]. There are few works in literature on the effect of others interstitial elements on the mechanical properties of high-Mn steels. In the last decades, it has been found that nitrogen affects the dislocation structure and deformation mechanisms, particularly twinning in Hadfield steels. This is attributed to the lowering of the intrinsic stacking fault energy (SFE) due to nitrogen addition, resulting in increased separation of partial dislocations required for twin nucleation [8].

It is well-known that nitrogen is a strong austenite stabilizer in stainless steels [9]. Additionally, it has been shown that nitrogen improves the mechanical properties [10] and corrosion resistance in this type of alloys [11]. However, the incorporation of nitrogen is a complex process, considering the low solubility of this element in liquid iron, which is only 0.045 wt.% at 1600°C and atmospheric pressure [12]. Usually, nitrogen levels above 1 wt.% can only be obtained through alloying and specialized high-pressure melting techniques [13]. However, the high-pressure melting technologies are complex, expensive, energy-consuming, and often difficult to control [14].

Mechanical alloying is a powder processing technique that involves the repeated cold welding, fracturing, and re-welding of a mixture of powder particles in a high-energy ball mill to produce a material with a controlled microstructure. This technique has been used to synthesize equilibrium and non-equilibrium materials such as amorphous alloys, nanocrystalline materials, intermetallic compounds, and supersaturated solid solution [15].

Few works in literature have addressed the influence of N_2 atmosphere on the microstructural and morphological evolution of the powders during the mechanical alloying process in the Fe-Mn-based system. In this context, Cisnero et al. [16] reported that it is possible to obtain a supersaturated solid solution of nitrogen when a Fe-18 wt. % Cr- 11 wt. % Mn powder mixture is subjected mechanically alloyed during 170 h in an Attritor mill under N_2 atmosphere. The high nitrogen concentration in solid solution was attributed to preferential accommodation at dislocation elastic stress fields, as well as at nanograin boundaries. Additionally, Tehrani et al. [17] studied the effect of particle size of iron powder on α-ferrite to γ-austenite transformation in Fe- 18 wt. % Cr- 10 wt. % Mn- 4 wt.% Mo stainless steel produced by mechanical alloying under N_2 atmosphere. They found that by decreasing the iron mean particle size, a higher α-ferrite to γ-austenite transformation rate is obtained due to the increase in the rate of nitrogen absorption in the powders during the milling process.

Although there are some studies that address the effect of N_2 on the mechanical alloying process of powders containing Fe and Mn, these have focused mainly on multicomponent systems associated with austenitic stainless steels. Until now, no studies have been conducted to determine the influence of N_2 atmosphere on the mechanical alloying process of Fe-Mn powders with a composition close to Hadfield steel. Considering the above, in the present work the N_2 effect on the mechanical alloying process and subsequent heat treatment of Fe-14 wt.% Mn powders was studied. In order to establish the individual effect of nitrogen as an interstitial element, it was decided not to incorporate carbon in this study.

MATERIALS AND METHODS

Fe powders (99.5 % purity, particle size less than 100 μm, Bioquímica) and Mn flakes (99.0 % purity, particle size less than 3 mm, Sigma Aldrich) were used as raw materials in milling experiments. Figure 1 presents SEM images of the starting powders. It can be seen that Fe particles have an irregular shape while the Mn flakes show a plate-like morphology.

The mechanical alloying process of 3.071 g of Fe powders and 0.500 g of Mn flakes was carried out in a SPEX 8000D mill using a cylindrical tungsten carbide vial with 20 hardened steel balls of 9.5 mm diameter. Additionally, 1 wt. % of stearic acid was used as a process control agent. A constant ball to powder ratio of 20:1 was maintained during all tests. The vials containing the powders and the balls were evacuated by a rotary pump and then back-filled with Ar (99.998 % purity, Linde Group) or N_2 (99.999% purity, Linde Group) in a glove box. The milling times employed were 1, 3, 5, and 10 h. The milling was performed discontinuously to minimize temperature rise caused by the mechanical alloying process, i.e., 0.5 h of milling followed by rest periods of 0.5 h. All the milling tests were done in duplicate to confirm the reproducibility of the results.

The microstructural and morphological evolution of the powders during the mechanical alloying process was studied by X-ray diffraction (Shimadzu, model XRD-6100, KαCu) and scanning electron microscopy (Zeiss, model EVO MA10). Furthermore, the particle size distribution was determined using laser diffraction (Malvern, model mastersizer Hydro 2000).

The thermal stability of the mechanical alloyed powders was studied by X-ray diffraction and differential scanning calorimetry in an SDT 650, TA instruments device. The differential scanning calorimetry analyses were carried out under gas flow (N_2 or Ar) of 50 mL min^{-1}, at a heating rate of 20°C min^{-1} between 50 and 1000°C.

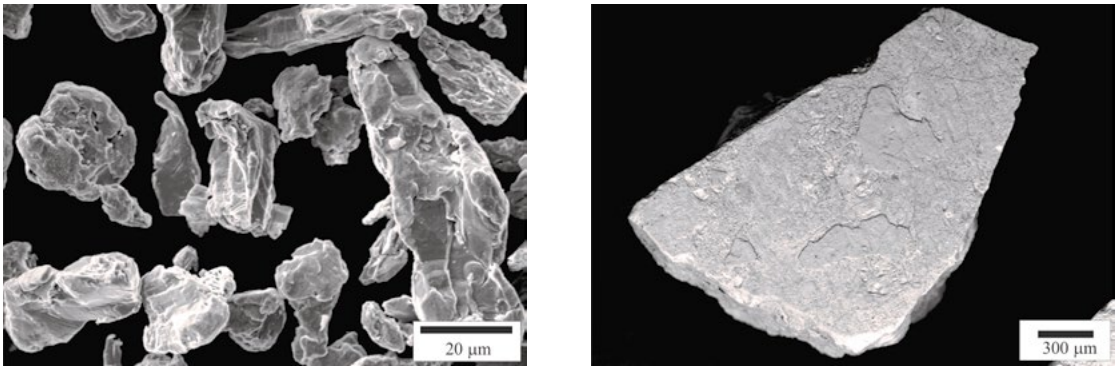

Fig.1 - SEM morphology of the starting powders: (a) Fe and (b) Mn.

RESULTS AND DISCUSSION

Figure 2 shows X-ray diffraction patterns of the Fe-14 wt.% Mn powders mechanically alloyed during 1, 3, 5, and 10 h under Ar and N_2 atmosphere. To compare the XRD patterns, they were normalized with respect to the maximum intensity. It is possible to observe that there is no important difference in the phase evolution during the mechanical alloying process carried out under Ar and N_2 atmosphere. It is appreciated that the relative peak intensity of Mn gradually decreases in both millings. Only traces of this element were found after 10 h. Additionally, the formation of α Fe-Mn solid solution during the first hour of milling was detected. The existence of α Fe-Mn solid solution was determined analyzing Figure 3, which shows the variation of the Fe lattice parameter regarding the milling time. It can be seen that during the mechanical alloying process carried out under Ar and N_2 atmosphere, the Fe lattice parameter gradually increases with the milling time. This fact would be related with the entry of the Mn atom inside the Fe structure during the mechanical alloying process. Similar results have been reported by Marinelli et al. [18] and Gebhardt et al. [19]. Concerning the milling atmosphere there is no clear effect on the lattice parameters of the α Fe-Mn solid solution. However, this change may be masked by the Mn effect due to the low nitrogen content that Fe can dissolve [20].

Examining the X-ray diffraction patterns in detail, it is possible to observe that the α Fe-Mn solid solution peaks present an asymmetry towards lower angles (Figure 4). This fact can be attributed to the formation of a second phase that has the same structure type as the bcc α Fe-Mn solid solution, but with a larger lattice unit volume. According

to literature [21], this new phase would be an oversaturated α Fe-Mn solid solution with a nominal composition of $Fe_{0.8}Mn_{0.2}$. It has been suggested that the energy stored in the powders caused by internal strains and the large grain boundary fraction due to the microstructural refinement produced by the mechanical alloying process can serve as a driving force for oversaturated solid solution formation [15]. In this way, two solid solutions of α Fe-Mn with different amounts of Mn in their structure would coexist in the mechanically alloyed powders.

Contrary to what was reported by Tcherdyntsev et al. [22], the presence of fcc γ Fe-Mn solid solution was not detected in this study. However, the possibility of its formation at longer milling times is not ruled out because it has been found that the $Fe_{0.8}Mn_{0.2}$ phase is a precursor of the γ Fe-Mn solid solution.

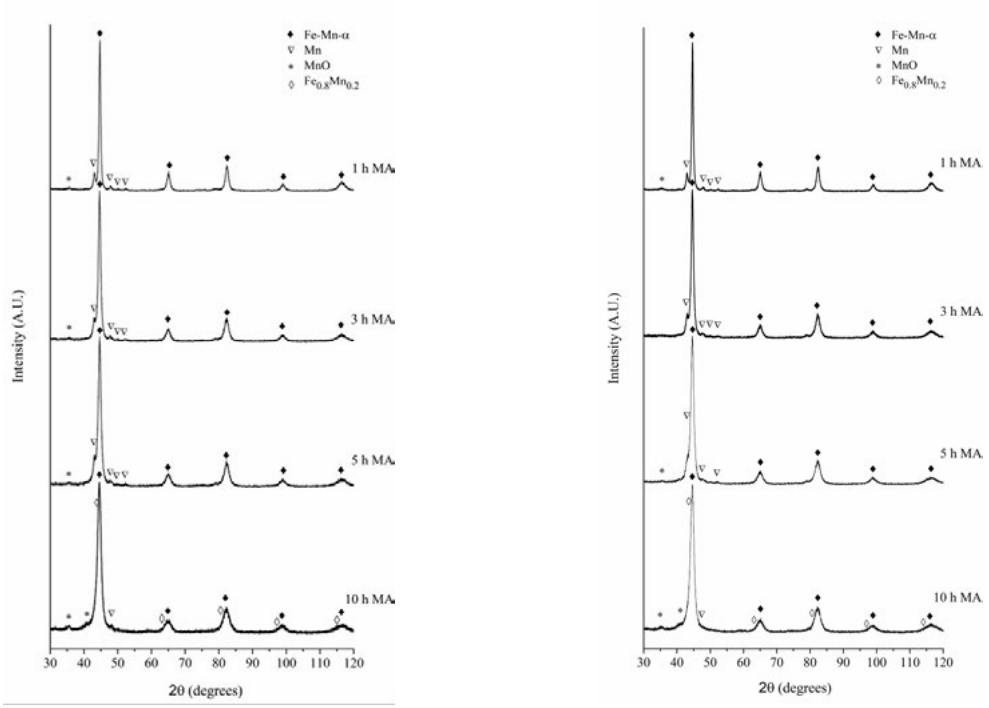

(a) (b)

Fig.2 - X-ray diffraction patterns of powders mechanically alloyed under (a) Ar and (b) N_2.

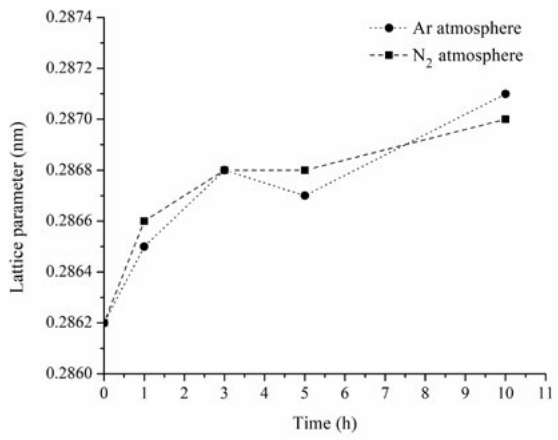

Fig.3 - Lattice parameter of α-Fe-Mn solid solution as function of milling time.

La Metallurgia Italiana
International Journal of the Italian Association for Metallurgy

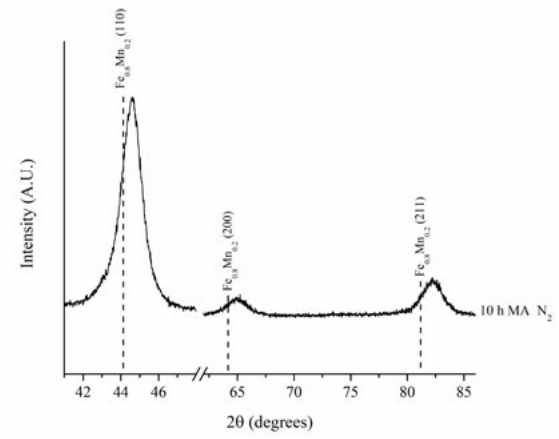

Fig.4 - X-ray diffraction pattern of powders mechanically alloyed during 10 h under N_2.

Figure 5 shows the variation of the average crystallite size of α Fe-Mn solid solution as function of the time for both millings. The average crystallite size was calculated from the (211) plane using Scherrer's formula [23]. It is observed that the milling atmosphere does not significantly affect the microstructure refinement of the powders. During the first 3 h the average crystallite size is rapidly reduced from 20 to 8 nm. After that, the rate of decrease of crystallite size is reduced due to the competition between the plastic deformation via dislocation motion that tends to decrease the crystallite size, and the recovery and recrystallization behavior of the material that tend to increase the crystallite size [24]. Similar results were found by Dorofeev et al. [25] and Duan et al. [26] for the Fe-Mn system.

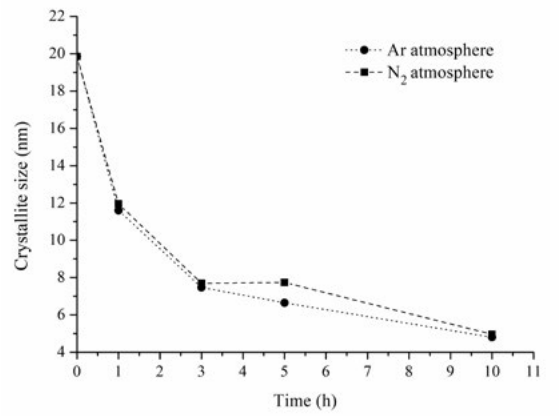

Fig.5 - Average crystallite size of α Fe-Mn solid solution as function of the time.

Figure 6 shows SEM images of Fe-14 wt.% Mn powders milled at different times under Ar and N_2 atmosphere. It can be observed that after the first hour of milling, the powders consist of flat agglomerates produced because of the ductile nature of Fe and Mn, which are plastically deformed. This morphology is characteristic of the initial stage of milling of ductile materials due to the strong plastic deformation and agglomeration of the powders [15, 17]. As the milling process proceeds, the capacity of particles to accept further plastic deformation decreases. The flat agglomerates are fractured, and the particles produced are welded together by cold deformation to form small agglomerates with rough surfaces. Concerning the effect of the milling atmosphere on the morphology,

it is possible to observe that there is only a difference in the initial stage of the mechanical alloying process, where the powders milled under Ar show a flatter morphology compared to the powders milled under N_2 atmosphere. This difference could be explained by considering the embrittlement effect of nitrogen in the Fe-Mn alloys [27].

To complement the morphological characterization of the powders during the mechanical alloying process, the particle size distribution was determined as a function of the milling time. Figure 7 shows a comparative plot of the size distribution for powders milled during 1 and 10 h. Additionally, the size distribution for raw Fe powders is presented for comparison. The results obtained corroborated the observations made by SEM. The powders milled for 1 h presented a wider particle size distribution than the raw Fe powders. This fact can be understood considering the formation of the agglomerates in the initial stage of the mechanical alloying process due to the high energy transferred by the milling media and the high ductility of the metallic powders. Consecutively, as the milling time increases, the particles are embrittled, and their size decreases.

To determine the phase distribution during the mechanical alloying process, powders with different milling times were metallographically prepared and observed by SEM. Figure 8 shows backscattered electron micrographs and corresponding EDS elemental maps of Mn. The results indicate that as the milling time increases, homogenization of the Mn distribution in the Fe matrix occurs due to the repeated cold welding, fracturing, and re-welding of powder particles during the mechanical alloying process. After 10 h of milling, no Mn-rich areas were detected. The elemental analyses confirm the formation of a solid solution of Fe- Mn, corroborating the X-ray diffraction results.

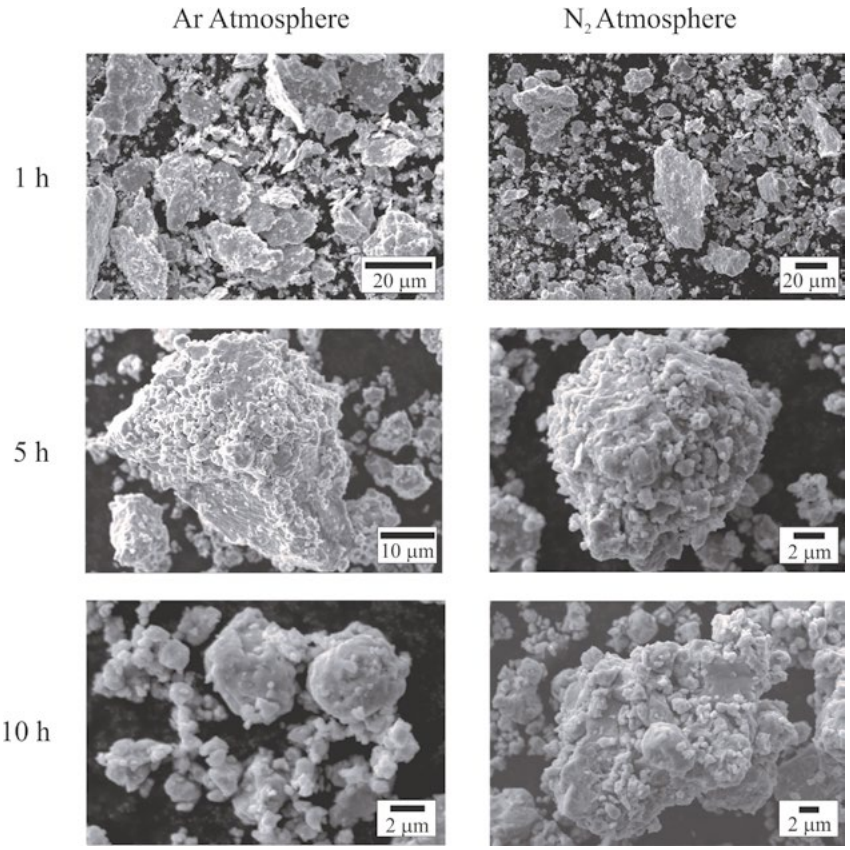

Fig.6 - Morphology of the powders mechanically alloyed under Ar and N_2 after 1, 5, and 10 h of milling.

La Metallurgia Italiana
International Journal of the Italian Association for Metallurgy

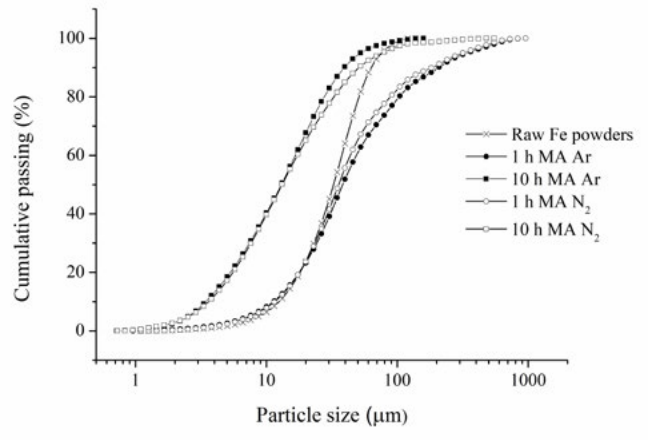

Fig.7 - Size distribution for powders mechanically alloyed under Ar and N_2 after 1 and 10 h of milling. The size distribution for raw Fe powders is presented for comparison.

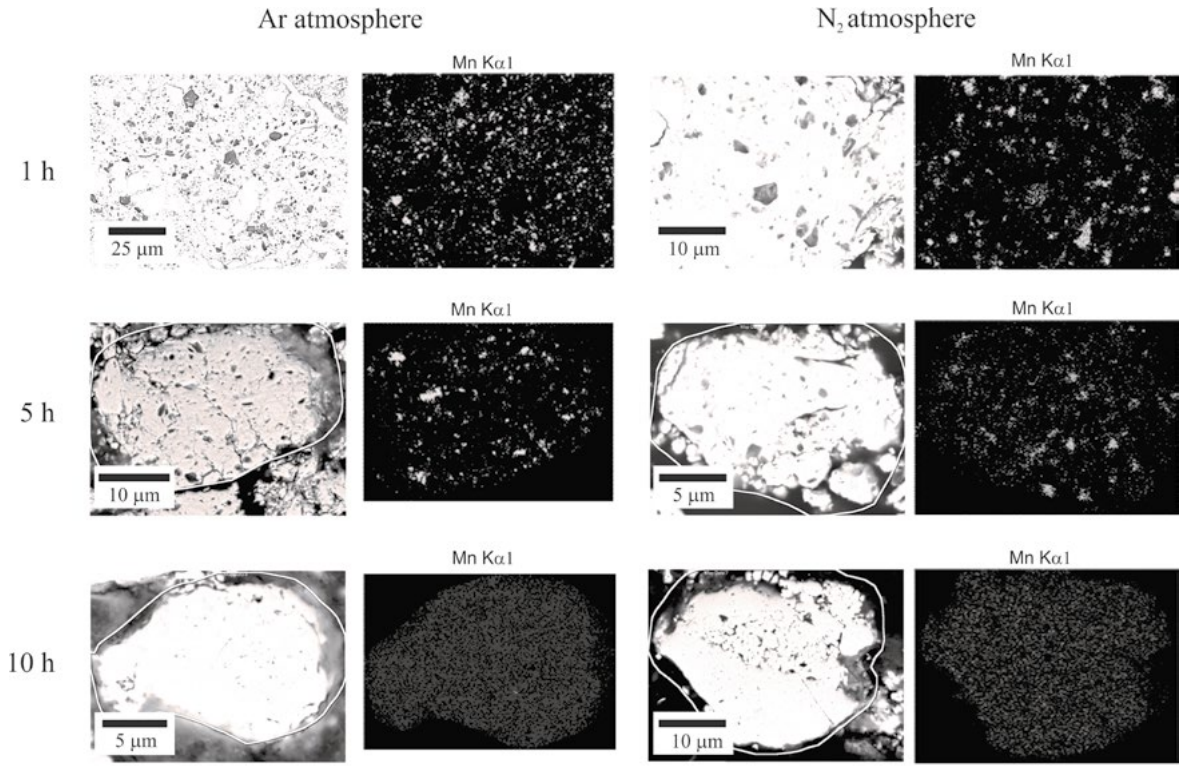

Fig.8 -Backscattered electron images of cross sectioned powders and corresponding EDS elemental maps of Mn.

Figure 9 shows DSC traces of the mechanically alloyed samples. The powders were analyzed under Ar or N_2 flow according to the atmosphere used during the milling. Two heating–cooling cycles were carried out to determine the reversibility of the processes. For both sets of samples, an endothermic reaction between 650 and 750 °C was detected. As can be seen in the tables inserted in the figures, the enthalpy change associated with this transition was higher for the powders analyzed under N_2 flow. On the other hand, contrary to what was observed in the powders milled under Ar, the initial reaction temperature for the powders analyzed in N_2 flow decreases with the

milling time.

Two heating steps were performed to determine the reversibility of the endothermic reaction. As an example, Figure 10 shows the first and second heating for the powders milled during 10 h under N_2 atmosphere; it is possible to observe in the second heating the same endothermic reaction detected during the first DSC analysis, which evidences the reversibility of the reaction under study.

To determine the origin of the endothermic reaction, the heated powders were analyzed by X-ray diffraction. The results are shown in Figure 11. It is observed that the heat treatment promotes the formation of fcc γ Fe-Mn solid solution. The relative intensity of the X-ray diffraction peaks of this phase becomes stronger when the powders are milled and heat-treated under N_2. This fact would be related to the greater relative quantity of γ Fe-Mn solid solution in these powders and would explain the higher heat absorbed by the samples treated under N_2 (Figure 9). Additionally, a great presence of MnO was detected in comparison with the mechanically alloyed samples due to the oxidation of remaining elemental Mn.

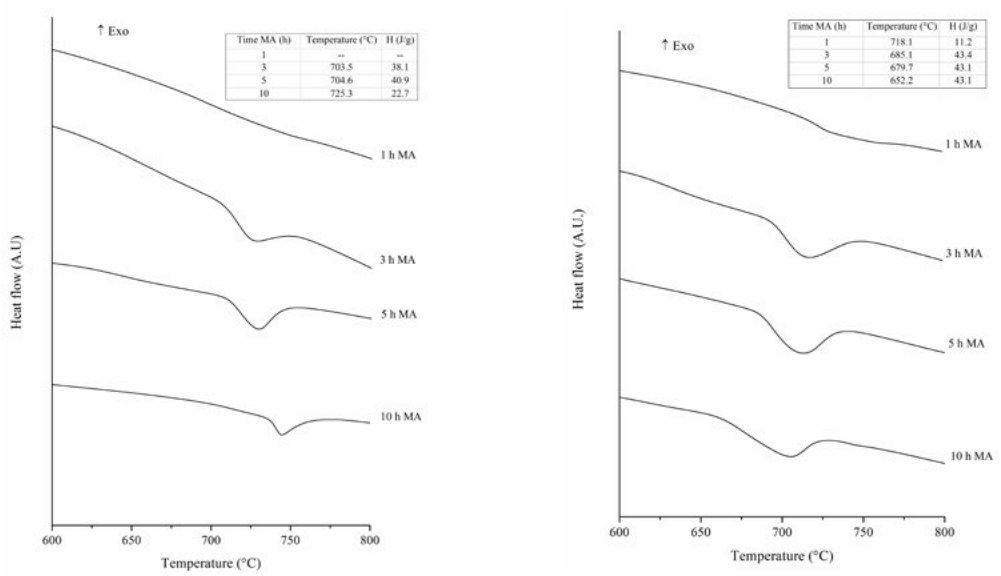

(a) (b)

Fig.9 - DSC traces of the powders mechanically alloyed under (a) Ar and (b) N_2.

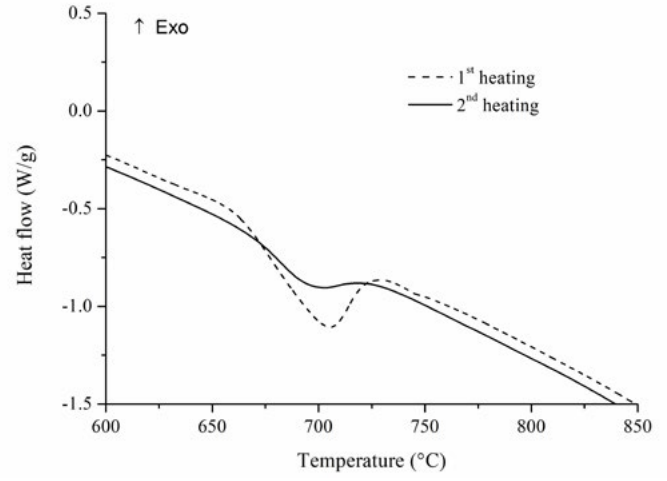

Fig.10 - First and second heating for the powders milled during 10 h under N_2.

Considering the results obtained and the phase diagram Fe-Mn reported by Witusiewicz et al. [28], it is possible to conclude that the endothermic reaction detected in the DSC analyses would be associated with the formation of γ Fe-Mn solid solution. Additionally, a larger presence of this phase in the powders milled and heat-treated under N_2 is observed (Figure 11). This behavior is coincident with the highest heat absorbed by these powders during the DSC analyses (Figure 9), and it agrees with the conclusions reported by several authors for stainless steels, where it was established that N tends to stabilize the austenitic solid solution [16, 17].

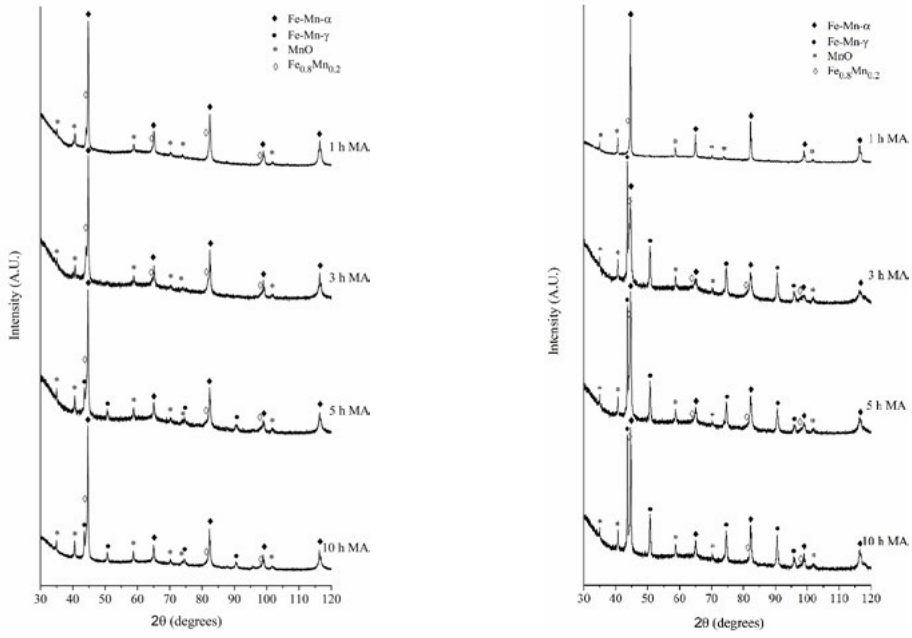

(a) (b)

Fig.11 - X-ray diffraction patterns of powders mechanically alloyed and heat-treated under (a) Ar and (b) N_2.

Regarding thermal stability of $Fe_{0.8}Mn_{0.2}$ solid solution, Figure 12 shows the comparison between X-ray diffraction patterns of the powders milled during 5 h and heat-treated under N_2. It is possible to observe that the diffraction intensity of $Fe_{0.8}Mn_{0.2}$ decreases during heating. This decrease could be associated with the appearance of γ Fe-Mn solid solution and confirms the important role that the $Fe_{0.8}Mn_{0.2}$ phase plays in the formation of γ Fe-Mn solid solution.

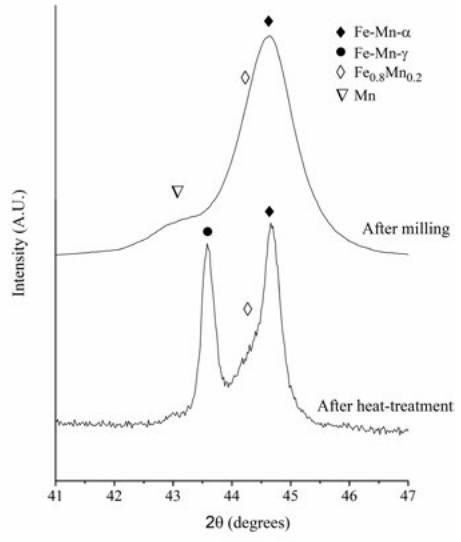

Fig.12 - X-ray diffraction patterns of the powders milled during 5 h and heat-treated under N_2.

CONCLUSIONS

The results indicated that the milling atmosphere (Ar / N_2) does not influence the phases detected after 10 h of mechanical alloying. After this milling time, the presence of two solid α Fe-Mn solutions with different manganese content was observed.

In terms of morphology, powders milled under Ar atmosphere presented a more lamellar aspect than powders milled in N_2 atmosphere. Regarding the distribution of sizes, it was determined that at initial milling times, a relative increase in the size of the agglomerates occurs as a result of the prevalence of the weld over the fracture. This trend is reversed to higher milling times.

Concerning the study of thermal stability of the mechanical alloyed powders, it was found that N_2 favors the formation of the γ Fe-Mn solid solution. Additionally, it was determined that the $Fe_{0.8}Mn_{0.2}$ supersaturated solid solution acts as precursor of γ Fe-Mn phase during the heating.

ACKNOWLEDGMENTS

This study was financially supported by DIUDA Iniciación [Project No. 22323]. The authors would like to thank the Department of Metallurgy of the University of Atacama for the XRD, SEM, and DSC analyses [Projects EQM 130125, EQUV 003, and EQUR 16002].

REFERENCIAS

[1] Hadfield R., 1883. High manganese steel. British Patent Nº 200.
[2] Lindroos M, Cailletaud G, Laukkanen A, Kuokkala V. Mat. Sci. Eng. A-Struct. 2018; 720: 145–159. https://doi.org/10.1016/j.msea.2018.02.028.
[3] Chen C, Bo L, Hua M, Dongyun S, Fucheng Z. Tribol. Int. 2018; 121: 389–399. https://doi.org/10.1016/j.triboint.2018.01.044.
[4] Grässel O, Krüger L, Frommeyer G, Meyer L. Int. J. Plasticity 2000; 16: 1391–1409. https://doi.org/10.1016/S0749-6419(00)00015-2.
[5] Sawaguchi T, Maruyama T, Otsuka H, Kushibe A, Inoue Y, Tsuzaki K. Mater. Trans. 2016; 57: 283–293. https://doi.org/10.2320/matertrans.MB201510.
[6] Chowdhury P, Canadinc D, Sehitoglu H. Mat. Sci. Eng. R 2017; 122: 1–28. https://doi.org/10.1016/j.mser.2017.09.002.
[7] Bayraktar E, Khalid F, Levaillant C. J. Mater. Process. Tech. 2004; 147: 145–154. https://doi.org/10.1016/j.jmatprotec.2003.10.007.
[8] Iglesias C, Solórzano G, Schulz B. Mat. Charact. 2009; 60: 971–979. https://doi.org/10.1016/j.matchar.2009.03.015.
[9] Reed R. JOM-J. Min. Met. Mat. S. 1989; 41: 16–21. https://doi.org/10.1007/BF03220991.
[10] Li H, Jiang Z, Zhang Z, Xu B, Liu F. J. Iron. Steel Int. 2007; 14: 330–334. https://doi.org/10.1016/S1006-706X(08)60105-3.
[11] Arya SB, Raja BS, Tiwari AN. Adv. Mat. Res. 2013; 794: 626–631. https://doi.org/10.4028/www.scientific.net/AMR.794.626.
[12] Satir-Kolorz AH, Feichtinger HK. Z. Metallkd. 1991; 82: 689–697.
[13] Simmons JW. Mat. Sci. Eng A-Struct. 1996; 207: 159–169. https://doi.org/10.1016/0921-5093(95)09991-3.
[14] Romanczuk E, Perkowski K, Oksiuta Z. Materials 2019; 12: 3416. https://doi.org/10.3390/ma12203416.
[15] Suryanarayana C. Prog. Mater Sci. 2001; 46: 1–184. https://doi.org/10.1016/S0079-6425(99)00010-9.
[16] Cisneros M, López H, Mancha H, Vázquez D, Valdés E, Mendoza G, Méndez M, Metall. Mater, Trans. A 2002; 33: 2139–2144. https://doi.org/10.1007/s11661-002-0045-1.
[17] Tehrani F, Abbasi MH, Golozar MA, Panjepour M. Mat. Sci. Eng A-Struct. 2011; 528: 3961–3966. https://doi.org/10.1016/j.msea.2010.12.043.
[18] Marinelli P, Baruj A, Guillermet AF, Sade M. Z. Metallkd. 2000; 91: 957–62.
[19] Gebhardt T, Music D, Hallstedt B, Ekholm M, Abrikosov IA, Vitos L, Schneider JM. J. Phys. Condens. Matter 2010; 22: 295402. https://doi:10.1088/0953-8984/22/29/295402.

[20] You Z, Paek M, Jung I. J. Phase Equilib. 2018; 39: 650–677. https://doi.org/10.1007/s11669-018-0666-8
[21] Sumiyama K, Nakamura Y, Ohshima N. Phys. Status Solidi A. 1986; 98: 229-238. https://doi.org/10.1002/pssa.2210980126.
[22] Tcherdyntsev VV, Pustov LY, Kaloshkin SD, Shelekhov EV, Principi G. Hyperfine Interact. 2006; 168: 937–942. https://doi:10.1007/s10751-006-9399-x.
[23] Scherrer P. Nachr. Ges. Wiss. Göttingen. 1918; 2: 98–100. https://doi.org/10.1007/978-3-662-33915-2_7.
[24] Ecker J, Holzer JC, Krill CE III, Johnson WL. J. Mater. Research. 1992; 7: 1751–1761. https://doi.org/10.1557/JMR.1992.1751.
[25] Dorofeev G, Lubnin A, Ulyanov A, Kamaeva L, Lad´yanov V, Pushkarev E, Shabashov V. Mater. Lett. 2015; 159: 493-497. https://doi.org/10.1016/j.matlet.2015.08.050
[26] Duan C, Chen C, Zhang J, Shen Y, Feng X. Power Technol. 2016; 294: 330–337. https://doi.org/10.1016/j.powtec.2016.02.048.
[27] Nasim M, Edwards BC, Wilson EA. Eng. A-Struct. 2000; 281: 56–67. https://doi.org/10.1016/S0921-5093(99)00734-0.
[28] Witusiewicz V.T, Sommer F, Mittemeijer EJ. J. Phase Equilib. Diff. 2004; 25: 346–354. https://doi.org/10.1361/15477030420115.

TORNA ALL'INDICE >